IEEE Access
Multidisciplinary | Rapid Review | Open Access Journal

Date of publication xxxx 00, 0000, date of current version xxxx 00, 0000.

Digital Object Identifier 10.1109/ACCESS.2017.DOI

An Energy-Efficient PAR-Based Horticultural Lighting System for Greenhouse Cultivation of Lettuce

AFAGH MOHAGHEGHI[1], (Student Member, IEEE), MEHRDAD MOALLEM[2], (Member, IEEE)
[1]School of Mechatronic Systems Engineering, Simon Fraser University, Surrey, BC, Canada (e-mail: amohaghe@sfu.ca)
[2]School of Mechatronic Systems Engineering, Simon Fraser University, Surrey, BC, Canada (e-mail: mmoallem@sfu.ca)

Corresponding author: A. Mohagheghi (e-mail: amohaghe@sfu.ca).

This research was supported in part by MITACS and the Natural Sciences and Engineering Research Council of Canada (NSERC) under the Discovery Grants Program.

ABSTRACT

This paper presents an intelligent horticulture lighting and monitoring system to achieve energy-efficient supplemental lighting while maintaining the light quality and intensity at desired levels in the photosynthesis spectrum. Energy-efficiency is achieved through delivering only the required net light intensity, consisting of sunlight and supplemental LED light, using an intelligent controller that does not depend on the lighting system model. To this end, an online neural-network learning control system is developed, comprised of low-cost light sensors for measuring the photosynthetic photon flux density (PPFD), dimmable LED light fixtures, cameras, and internet-of-things (IoT)-enabled firmware used for crop monitoring and performance evaluation. Experiments performed in a research greenhouse facility on the lettuce crop are presented which indicate that the system can deliver the desired Daily Light Integrals (DLIs) to the plants in the presence of changing daylight conditions. The proposed method can thus deliver the exact amount of light to a specific crop based on the required light recipes during different growth phases. The control performance is further compared with a conventional on-off time-scheduling method in terms of plant health, growth, and energy requirements. The experiments indicate that the proposed solution can reduce energy consumption per unit dry mass of lettuce by 28% when compared to existing time-scheduling methods.

INDEX TERMS Daylight Harvesting, Energy-efficiency, Horticultural Lighting, Internet-of-Things, Machine Learning, Neural Networks, PAR Measurement.

I. INTRODUCTION

Supplemental lighting is used to increase the daily light exposure of crops in greenhouses located in northern latitudes. To improve plant growth, yield, and quality while minimizing electricity consumption of artificial lighting, it is desirable to utilize the freely available sunlight as much as possible [1]. Thus, there is a great incentive to incorporate innovative technologies into today's greenhouse lighting automation systems. The emergence of horticultural light-emitting diodes (LEDs) has facilitated this integration when compared to traditional horticulture light sources such as metal halide (MH) and high pressure sodium (HPS). Horticultural LEDs can further deliver dimmable light in the photosynthetic spectrum and can readily be incorporated into digital control systems, allowing for lighting schemes to be tailored to the plants' needs. Considering the plants' sensitivity to light, the photosynthetically active radiation (PAR) flux density is defined as the light energy in the 400-700nm spectrum, referred to as the photosynthesis band, measured in $\frac{W}{m^2 s}$ [2]. However, photosynthesis is a quantum process that is more dependent on the received number of photons than their energy [3]. In relation to plant growth and morphology, PAR is measured in terms of the flux of photons per unit area, or Photosynthetic Photon Flux Density (PPFD), expressed in $\frac{\mu mol}{m^2 s}$.

Horticultural lighting has traditionally concentrated on issues such as yield quality, quantity, and experimental crop-specific light recipes involving light intensity, spectrum, and photoperiod. In this respect, intelligent methods for precise delivery of the required light recipe, while minimizing energy consumption, has received increasing attention in recent years. A discussion of pertinent literature and existing chal-

lenges is presented in the following along with the contributions of the present work.

Horticultural LED lighting and its effects on crop growth have been investigated by several authors [4]–[14]. Research on LED crop lighting dates back to the 1980's, with red-only lights used in the international space station, to high-density multi-spectral LED chip-on-board devices in recent years [4], [5]. An early work by Albright *et al.* [7] showed that dry mass accumulation is proportional to the daily light integral (DLI) and a consistent DLI is central to quality crop production. Later studies have shown that plant growth and development (e.g., flower-bud initiation, inter-node length, branching, leaf area) and crop production value (yield, vitamins, pigments) are directly affected by lighting [8]–[11]. In [12], the authors provided an overview of the effects of LED lighting on the growth, yield, and nutritional quality of green leafy vegetables, fruits, and ornamental plants. In [13], the authors discussed how spectral quality of LEDs can dramatically affect crop anatomy, morphology, nutrient uptake, and pathogen development. In [14], an adjustable spectrum LED was presented to match the plant's spectrum based on the relative quantum efficiency [2]. In [15], the authors provided a review of research activities related to LED lighting and highlighted issues such as plant cultivar-dependent recipes and cost analysis.

The studies in [16]–[29] demonstrate how dynamic lighting and optimization methods can help to increase the energy savings achievable by LED systems. In [17], the effects of dynamic regulation of supplemental lighting intensity on electricity consumption and fresh weight buildup were examined. The study in [18], analyzed the growth of an ornamental crop under dynamic regulated LED lighting. The data from a quantum PAR sensor was used to incrementally increase/decrease the LED light intensity to within a 10% tolerance. The results indicated a 21% energy reduction. However, no difference in crop quality, or time to anthesis, was observed and the method is open-loop and not robust to parametric variations and disturbances. In [20], the authors examined lettuce cultivation using red and blue LEDs. The plant's growth was represented in a feed-forward network using an image segmentation method based on K-means clustering. The paper reported 40-52$\%$ reduction of energy and an increase the leaf area by up to 6%; however, it was done in a simulated scenario with no experimental results. In [21], [22], the researchers investigated spectrum controlled and targeted LED lighting to achieve energy savings. Through targeted plant lighting and spectral optimization, a 50% reduction in energy usage per unit of dry biomass was achieved. However, the comparison for energy savings was with traditional inefficient horticultural lights such as HPS and MH technologies.

In [27], a herbal remedy plant was grown under natural light and under LED fixtures with varying light conditions. Simulation of multiple spectra showed that the method could replicate the intended spectrum with minimum fitness errors. However, the study did not report energy saving amounts. In [28], the LED light intensity was optimized over time for different electric energy and lettuce crop prices, but was restricted to simulations in a plant factory with no daylight harvesting. In [29], the authors presented existing energy-saving methods using LEDs in plant factories. The plant canopy image was captured during different growth stages and appropriate LEDs above the plant were turned on to avoid light wastage. At the same time, the on-time and brightness levels of LEDs were calculated to produce the required light profile. This study focused on spatial configuration of the LEDs for energy saving but used an on-off method for intensity control which has limitations in terms of energy-savings and light quality as presented in this paper. In [30], the authors investigated lettuce cultivation in an indoor farming setup exposed to red and blue LED lights using an image segmentation method, based on K-means clustering, to identify and optimize the lighting schedule. However, this work did not have an energy harvesting focus through daylighting.

The above works have presented interesting results related to yield increase and energy saving potential of dynamic LED lighting schemes. However, they mostly suffer from certain issues in their sensing and control schemes. For instance, quantum PAR sensors are very costly to deploy in large numbers in a greenhouse environment. Meanwhile, primitive light sensors only allow for color ratio control and not PAR control. Furthermore, the control and optimization algorithms used in previous works are mostly very simple and highly dependent on the system model. In a horticultural system, both the light environment and daylight contribution change with plant growth and seasonal and weather conditions. Thus, model-based methods would not have acceptable performance since the environmental parameters change with time, leading to variations in the system model and hence deteriorated closed-loop control performance. Another drawback of model-based approaches is that they are not scalable since the system model changes with system size. Also, there is little evidence of research that utilizes both dynamic lighting for energy-efficiency and independent set-point light intensity regulation and control of color ratios.

The contribution of present work is addressing some of the above issues in horticultural lighting through utilizing machine learning-based light intensity sensing, using newly introduced low-cost spectral light sensors, combined with a learning neural network controller that does not depend on the mathematical model of the lighting system. To this end, a comparative study of machine learning methods for mapping the sensors readings to PPFDs is presented and experimentally tested in an IoT-based feedback control system. The controller can operate with minimal tuning to deliver canopy-level desired light recipes. The proposed system achieves cross-color-channel and cross-light-source illumination capability, leading to further improvement energy consumption and yield when compared to on-off time scheduling methods. A by-product of providing accurate light intensity in each spectrum would be to avoid plant health issues such as tip-

burn due to excessive light exposure.

The rest of this paper is organized as follows. Section II formulates the lighting control problem. Section III introduces the proposed solution including the IoT control system platform, estimation of PAR measurements using low-cost spectral light sensors, and the learning neural controller. Section IV presents the experimental setup used to evaluate performance of the proposed system. Section V presents the results of conducted experiments in a greenhouse facility. Conclusions and future work are presented in section VI.

II. PROBLEM FORMULATION

Reducing the cost of electricity for supplemental lighting to promote photosynthesis is desirable from an economic perspective. Supplemental lighting in the blue and red spectrum is the preferred method to maximize photosynthetic activity and minimize energy usage. Since the red:blue ratio of light received by plants would directly affect plant growth, dimmable blue and red light fixtures have been developed to achieve desirable light recipes ([31], [32]).

Using a two channel LED fixture to supplement light in the blue and red spectrum, it is necessary to have PAR sensors that can measure these colors separately, instead of the full photosynthetically active spectrum. Thus, we define two parameters for the photosynthesic photon flux density (PPFD) in the red and blue spectra, called $PPFD_r$ and $PPFD_b$, respectively. These parameters are defined as the number of photons in the 600-700nm and 400-500nm, respectively, that reach a surface area per unit of time (measured in $\frac{\mu mol}{m^2 s}$). The Daily Light Integral (DLI) is often used in plant growth and morphology. Thus, let us define the corresponding DLI parameters as DLI_r and DLI_b, which are the daily flux of photons in the 400-500nm and 600-700nm range per unit area, respectively (measured in $\frac{mol}{m^2 d}$). The conventional PAR measures of in the full 400-700nm photosynthesis spectrum are denoted by $PPFD_{full}$ and DLI_{full} throughout the rest of this paper.

The system model, consisting of n light fixtures with two color channels per fixture to control the PPFD levels of red and blue at n target points can be represented by a linear, static, time-invariant MIMO system in the following form

$$y(t) = Tu(t) + y_L(t) \tag{1}$$

where $y(t)$ is the $2n \times 1$ output vector representing spectrum-specific PPFD readings at points of interest and is defined as

$$y(t) = \begin{bmatrix} PPFD_{r,1} \\ PPFD_{b,1} \\ \dots \\ PPFD_{r,i} \\ PPFD_{b,i} \\ \dots \\ PPFD_{r,n} \\ PPFD_{b,n} \end{bmatrix} \tag{2}$$

in which $i = 1, ..., n$ indicates the number of each sensor placed at a target point, and the subscripts r, b stand for red and blue spectral readings, respectively.

The $2n \times 1$ control input vector, $u(t)$, represents the dimming commands (0-100%) for the red and blue channels of LED fixtures as follows

$$u(t) = \begin{bmatrix} u_{r,1}(t) \\ u_{b,1}(t) \\ \dots \\ u_{r,i}(t) \\ u_{b,i}(t) \\ \dots \\ u_{r,n}(t) \\ u_{b,n}(t) \end{bmatrix} \tag{3}$$

where $i = 1, ..., n$ indicates the number of each two-channel light fixture, and the subscripts r, b stand for red and blue channel input commands of each fixture, respectively. Matrix T $(2n \times 2n)$ is a full-rank system matrix and y_L $(2n \times 1)$ is the vector of daylight contribution, modeled as an additive output disturbance. The system matrix T represents a cascade connection of three subsystems, namely, LED fixtures, LED drivers, and mapping between the emitted flux by light fixtures and light intensity at sensor locations from direct and reflected light rays [33].

III. SYSTEM COMPONENTS

In this section we present the proposed system which utilizes data from multiple light sensors positioned at crop levels to estimate the PAR received at the plant canopy and provides supplemental lighting through dimmable, multi-channel horticultural LED lights.

A. IOT PLATFORM

An IoT-enabled supplemental lighting control platform was designed and implemented consisting of the following components:

- *Light Sensing:* The multi-channel spectral light sensor AS-7341 (from ams-OSRAM) was used to sense light intensity. The spectral response of this sensor is defined by 11 individual channels covering 350-1000nm, with 8 channels centered in the visible spectrum (VIS), plus one near-infrared (NIR), and a clear channel. The SS-110 spectroradiometer (from Apogee Instruments) was used as a reference module for PAR data collection and sensor calibration. The SS-110 continuously measures lighting within the wavelength range of 340-820nm. It can be utilized for measurement of spectral output (energy flux density, photon flux density, or illuminance) of different radiation sources.
- *Supplemental Horticultural LED Lights:* Wireless controlled LED fixtures (Q400 from QuantoTech Solutions, Ltd.) allow dimmable red and blue light color intensities. The LED unit delivers a maximum PPFD output of 480 µmol/s and consist of 7W blue LED (460nm), 14W red LED (660nm) and 2W UV LED (385nm).

The wireless-enabled LED fixtures can be controlled through a local WiFi network using a RESTful API architecture. The WiFi module on the light fixture joins the local network with a self-defined IP address assigned automatically and allows for a controller connected to the same network to call for connection and transmit control commands.

- *Image Sensor:* A low-cost Raspberry Pi Camera Module v2 was used with an 8 mega-pixel camera based around the Sony IMX219 image sensor, which is capable of producing 3280×2464 pixel static images and a $640 \times 480p90$ video. With physical size of $25mm \times 23mm \times 9mm$ and optical size of $1/4$", the sensor is attached to, and controlled by, a Raspberry Pi unit by way of a dedicated Camera Serial Interface port (CSI).
- *Controller:* A Raspberry Pi 3 B+ was used with a BCM2837B0 System-on-Chip (SoC) and 1.4 GHz ARM Cortex-A53 processor running a Debian-based Linux distribution called Raspbian OS. This module is responsible for collecting sensor lighting data, using the machine learning trained PAR model, executing the control algorithm, and sending dimming commands to LED fixtures in real time. It is also in charge of setting image sensor configurations, timing and triggering captures, pre-processing of images, and authenticating and uploading the data to a cloud storage service for further analysis.
- *Cloud storage:* The Google service was used to store the image data along with their meta-data. The Raspberry Pi node device contains the code for using the Google Drive API to authenticate the Google account credentials and upload the data.
- *Processing and Analytics:* A desktop PC was used as the main processing unit for machine learning model fitting and image processing tasks to allow for powerful and cost-effective image processing and machine learning computations, and to verify performance of the lighting control scheme. The data was accessed on the cloud server, read into corresponding algorithms, and processed. The results were sent back to the Raspberry Pi for model/algorithm updates, uploading to the cloud, presentation on the PC, and feeding the ThingSpeak platform (from Mathworks, Inc).

B. LIGHT SENSOR CALIBRATION

Conversion of raw incident light data using the multi-spectral AS-7341 sensor to PPFD parameters was conducted using multiple machine learning algorithms including multi-linear regression, neural network, decision tree, and random forest. The details are not presented here due to space limitations. A very large data-set was created by collecting synchronized lighting data from AS-7341 (from amsOSRAM) along with the SS-110 spectroradiometer (from Apogee Instruments) throughout a year in SFU Surrey Campus, British Columbia, Canada (geo-location: 49.276765 -122.917957). Different weather conditions, geometrical configurations and supplemental lighting levels were considered in the data-set. Various linear and nonlinear regression models were used to fit the data. Although nonlinear regression models such as *random forest model* obtained more accurate results, the trade-off between simplicity and accuracy makes a multiple linear regression model the best choice for real-time control applications such as ours.

C. SUPPLEMENTAL LIGHTING CONTROLLER

As established in [32], a learning neural controller can harvest daylight and regulate light levels while eliminating the need for system identification, i.e., obtaining the system matrix T in (1). The adaptive nature of the control scheme also results in compensation of any uncertainty, or changes in the system model T, by the controller. Furthermore, the proposed method does not require any knowledge of the daylight term y_L.

The proposed neural network controller input presented in [32], is as follows

$$u(t) = N\, y_{da} \tag{4}$$

where $N \in R^{(2n+1)\times(2n+1)}$ represents the weight matrix for the neurons of a single layer neural network with the same number of nodes as outputs. The terms $y_{da} = \begin{bmatrix} y_d & 1 \end{bmatrix}^T$ is an augmented desired output vector with $y_d \in R^{(2n+1)\times 1}$, representing the desired output with the term 1 being a unit firing threshold bias. Note that each neuron uses an identity linear activation function. The proposed update law for evolution of weights is as follows

$$\dot{N} = k\, \varepsilon\, y_{da}^T - \eta \|\varepsilon\| N \tag{5}$$

where ε is the output error defined as

$$\varepsilon = y_d - y \tag{6}$$

and k, η, $\|.\|$ are positive scalar design parameters the Euclidian norm, respectively.

As discussed in [32], the closed-loop system with the proposed neural network controller is uniformly ultimately bounded if the following conditions hold

$$\frac{T + T^T}{2} \geq 0 \tag{7}$$

$$\|N\|_F \geq \frac{k\|y_{da}\|}{\eta} \tag{8}$$

$$k\underline{\sigma}_T \geq \eta \|T\| \|N\| \tag{9}$$

where $\|.\|_F$ denotes the Ferobinious norm and $\underline{\sigma}_T$ represents the smallest singular value of T. Moreover, the ultimate bound on the output error can be made arbitrarily small using the design parameters k and η as long as conditions (7),(8),(9) are satisfied.

The PPFD-based control system flowchart is provided in Fig. 1, in which the error signal to the neural network controller is obtained using the desired and actual PPFDs for red and blue channels. The desired PPFDs are obtained based on a target crop-dependent light recipe including daily

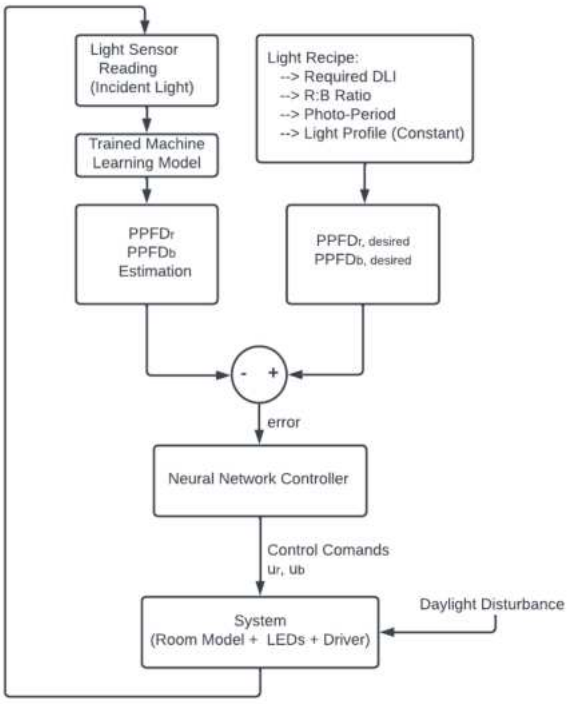

FIGURE 1. Flowchart of the PPFD-based neural-network lighting controller.

light integral (DLI), desired red to blue color ratio (R:B), photo-period, and a light profile (e.g., a constant daily value based on the crop development stage). The light sensor uses trained machine-learning coefficients to obtain PPFD in the red and blue channels and feeds them to the error block. The controller then obtains the dimming commands and applies them to the LED red and blue channels.

IV. EXPERIMENT DESIGN

A comparison experiment was designed to evaluate the performance of the proposed lighting control system and analyze its effects on plant health and growth.

A. EXPERIMENTAL SETUP

A greenhouse compartment as shown in Fig. 2 was utilized in the Institute for Sustainable Horticulture (ISH), Kwantlen Polytechnic University (KPU), Langley, BC, Canada (geo-location: 49.109619242053256, -122.64535537470125). Two systems were installed side by side, each consisting of two light sensors, two LED fixtures, and an independent controller: System 1 (Fig. 2 on the right), ran a time-scheduling on-off controller, and System 2 (Fig. 2 on the left) ran the proposed neural network controller.

TABLE 1. Nutrient solution recipe in PPM

N	P	K	Ca	S	Fe	Mn	B	Zn	Cu	Mo
240	50	350	160	67	0.9	0.55	0.23	0.33	0.05	0.05

FIGURE 2. Picture of KPU mini-greenhouse set-up for comparative experiments.

B. IRRIGATION AND NUTRIENTS

The two systems were built side-by-side on the same grow tray and shared the same hydroponic nutrition and water delivery system to keep nutritional conditions consistent. A drain to waste hydroponic system was utilized to provide water and nutrients to plants. The nutrient solution recipe, in parts per million (ppm), is shown in Table 1. Electrical Conductivity (EC) and pH of the nutrient solution were fixed at 2.0 mS/cm and 5.8, respectively. The temperature of nutrients was kept at approximately 19°C. The ambient temperature of the greenhouse varied in the range 18-20°C. The utilized irrigation schedule varied from a one-minute pulse twice a week, to two pulses of 1.5 minutes, every other day, using irrigation drippers with a capacity of 2 liters per hour.

C. CROP SELECTION

A green mini romaine organic lettuce variety, called Dragoon (LATIN NAME: Lactuca sativa), was selected. This variety is found, based on the producer's trials [34], to be a great performer in a climate-controlled greenhouse environment and suitable to be grown successfully using hydroponic growing methods, or other soil-less growing systems. The number of days to maturity for this variety is 43 for transplants, and 47 days for direct seeding, but can be sown every 2–3 weeks for a continuous supply of either full heads or baby leaves.

D. LIGHTING PLAN

An accurate lighting plan was created for the neural network system (System 2) to deliver the required DLI to the plant canopy according to a precise light recipe (red to blue PPFD ratio and photoperiod). Based on the required DLI, photoperiod, and red:blue ratio, and assuming a uniform daily light profile (constant PPFD throughout the day), the PPFD set-points for red and blue spectral ranges were obtained. Table 2, shows the obtained PPFD set-points based on provision

of 15.12 $\frac{mol}{m^2 d}$ daily light integral through supplying constant red and blue PPFDs to the plants during a 12 hour period from 7AM to 7PM. The selected target DLI was designed to promote healthy plant growth while preventing health issues such as tipburn according to previous studies [35], [36]. A red to blue ratio of 4:3 was selected as the most suitable spectra for the selected crop based on previous works [37], [38]. The light plan for the time scheduled system (System 1) was selected to represent the traditional on-off method used by growers for comparison of energy consumption and plant health properties. Both the red and blue channels of LED fixtures were turned on to full power (7W blue channel (460nm), and 14W red channel (660nm)) with a 12 hour photoperiod between 7AM and 7PM. In this case, the light source red/blue ratio was 2:1.

TABLE 2. Lighting plan for the neural-network controller (System 2).

DLI ($\frac{mol}{m^2 d}$)	15.12
R/B Ratio-L_{rb}	4:3
Photoperiod-T_p (hrs)	12
Start time	7AM
End Time	7PM
$PPFD_r$ ($\frac{\mu mol}{m^2 s}$)	200
$PPFD_b$ ($\frac{\mu mol}{m^2 s}$)	150

E. LIGHTING DATA COLLECTION

Two light sensors corresponding to the two LED fixtures were utilized to collect lighting data in real time. The sensor mount heights were selected to provide sufficiently accurate measurement of light received by the plants but were not shaded by the canopy as the plants grew. The SS-110 spectroradiometer (from Apogee Instruments) was placed close to one of the sensors in System 2, which collected 340-820nm spectral data continuously to provide a reference for PPFD measurements by the machine-learning calibrated sensors.

F. IMAGE DATA COLLECTION

An image sensor was located on top of each plant canopy beside the LED fixtures to collect image data. Periodic top view images were captured four times a day at 8AM, 14PM, 18PM, and 23PM under white light conditions. The system automatically turned the red and blue channels of the fixtures off and the white light on, captured images, saved them to the database, and resumed providing supplemental lighting. The image data was later processed using the PlantCV open source software [39] to extract color and geometrical features and monitor plant health and growth.

V. EXPERIMENTAL RESULTS

A. PPFD TRACKING RESPONSE

The tracking responses of the proposed neural-network system when compared to the time-scheduling system throughout a sample day in the grow cycle (Nov 21, grow cycle day 31) are illustrated in Figs. 3, 4, and 5, corresponding to $PPFD_r$, $PPFD_b$, and $PPFD_{full}$, respectively. The importance of this result is that, in addition to DLI requirements, plant health and growth was improved due to the uniformity and consistency of light profile received throughout each day. In Tables 3 and 4, a comparative analysis of Systems 1 and 2 for the sample day of the growth cycle is presented in terms of error between the desired and measured PPFD at plant canopy along with the energy savings for red, blue, and full PPFD, respectively.

Fig. 3.a, shows the tracking response for the average $PPFD_r$ of sensors in System 2 between 7AM and 7PM. Fig. 3.b displays the corresponding average dimming percentage for LED fixtures of System 2. It can be observed from Fig. 3.a, 3.b that, using the proposed controller, the 200 $\frac{\mu mol}{m^2 s}$ set-point for red PPFD is tracked with 0.3% error. To achieve this set-point, the red channels of LED fixtures were turned ON to a maximum value of 86% of their full power, resulting in an average of 32% energy savings on the red channel supplemental lighting for this day. Figs. 3.c, 3.d, illustrate the average $PPFD_r$ of the sensors and the red channel dimming percentage of LED fixtures for System 1. In this case, the panels are always 100% ON during the photoperiod with no savings in energy. Additionally, the red PPFD tracking error is at a very high value of 50%, resulting in the plant canopy to receive excessive red light which can result in plant health issues due to excessive light such as tipburn.

Fig. 4.a demonstrates the tracking response for the average $PPFD_b$ of sensors in System 2 throughout the day while Fig. 4.b represents the average dimming percentage of its LEDs. Referring to Figs. 4.a, 4.b, the 150 $\frac{\mu mol}{m^2 s}$ set-point for blue PPFD is tracked with 0.4% error. To achieve this level of precision in the blue spectral range, the blue channels of LED fixtures were turned ON to a max of 87% of full power to save an average of 33% in energy on the blue channel supplemental lighting for this day. Figs. 4.c, 4.d, indicate the average $PPFD_b$ of sensors and the dimming percentages of blue channel for System 1. In this case, the panels were always ON at 100% power during the photoperiod, resulting in no energy savings. Additionally, the blue PPFD tracking error were very high at 49%, exposing the plant canopy to an excessive amount of blue light, which might cause plant health problems.

Fig. 5, portrays similar information as in Figs. 3, 4 for $PPFD_{full}$. In System 2, the 350 $\frac{\mu mol}{m^2 s}$ set-point for full PPFD was regulated with 14% error. In comparison, the full PPFD tracking error for System 1 was a staggering 43%.

TABLE 3. PPFD tracking errors on day 31 for the two systems.

	MAE		MAPE		MSE		RMSE	
	Sys 1	Sys 2	Sys 1	Sys 2	Sys 1	Sys 2	Sys 1	Sys 2
$PPFD_r$	100	0.6	50%	0.3%	11784	2	109	1
$PPFD_b$	73	0.6	49%	0.4%	6975	3	84	2
$PPFD_{full}$	151	49	43%	14%	36725	3211	192	57

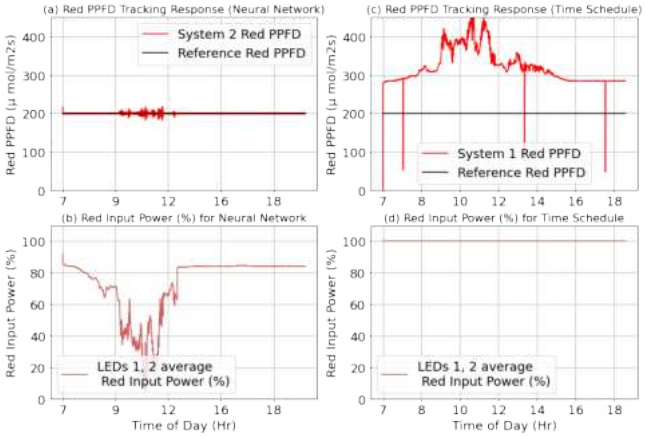

FIGURE 3. Red PPFD tracking response for neural-network and time scheduling controllers.

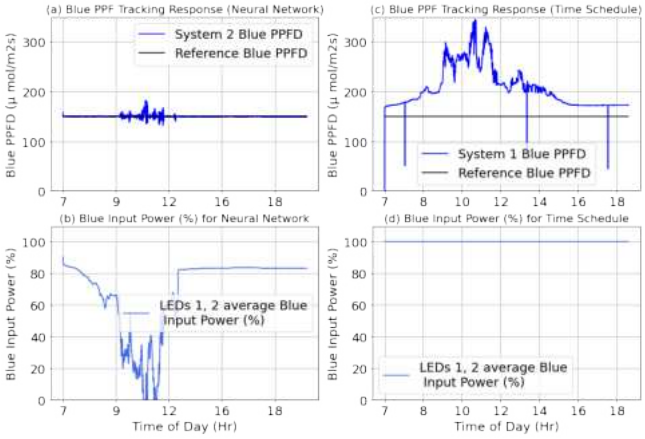

FIGURE 4. Blue PPFD tracking response for neural-network and time scheduling controllers.

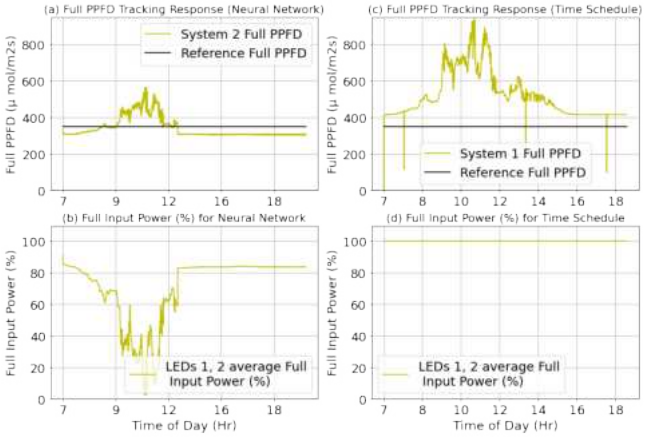

FIGURE 5. Full PPFD tracking response for neural-network and time scheduling controllers.

TABLE 4. PPFD energy savings comparison of the two systems on day 31.

	Ave		Min		Max	
	Sys 1	Sys 2	Sys 1	Sys 2	Sys 1	Sys 2
Red channel savings	0%	32%	0%	14%	0%	91%
Blue channel savings	0%	33%	0%	13%	0%	100%

B. DLI TRACKING RESPONSE

A comparison of the received DLIs at plant canopy levels and the corresponding LED fixture dimming levels (representing the energy used) for Systems 1 and 2 is depicted in Figs. 6, 7, and 8 for red, blue, and full spectral ranges, respectively.

The DLI is calculated from daily PPFD sensor readings by adding up all the collected samples as follows

$$DLI_{r/b/f} = \sum_{t=0}^{T_p \times 3600} PPFD_{r/b/f}(t) \qquad (10)$$

where $PPFD_{r/b/f}(t)$ denotes the red, blue or full PPFD sample collected at time t, assuming that one sample is collected every second.

In Table 5, a comparison of mean absolute error (MAE), mean absolute percentage error (MAPE), mean squared error (MSE) and root mean squared error (RMSE) of achieved DLIs in Systems 1 and 2 is presented. Table 6 presents the average, minimum, and maximum of energy savings. Examining the MAPE column in Table 5 reveals that the proposed neural network controller can reduce the mean absolute percentage error from 61% to 14% for red, from 40% to 16% for blue, and from 44% to 19% for full PPFD, respectively. From Table 6, it can be concluded that this error reduction is achieved with an average energy savings of 32% and 27% in the red and blue channels, respectively. It is worthwhile noting that the above percentages have increased to 80% and 55%, on certain days, depending on the specific daylight and weather conditions.

TABLE 5. DLI tracking errors for the full growth cycle (55 Days).

	MAE		MAPE		MSE		RMSE	
	Sys 1	Sys 2	Sys 1	Sys 2	Sys 1	Sys 2	Sys 1	Sys 2
DLI_r	5	1	61%	13%	45	4	7	2.05
DLI_b	3	1	40%	16%	7	3	3	2
DLI_{full}	7	3	44%	18%	73	15	9	4

TABLE 6. DLI energy savings comparison of the two systems for full growth cycle (55 Days).

	Ave		Min		Max	
	Sys 1	Sys 2	Sys 1	Sys 2	Sys 1	Sys 2
Red channel savings	0%	32%	0%	11%	0%	79%
Blue channel savings	0%	27%	0%	11%	0%	54%

C. PLANT HEALTH AND YIELD COMPARISON

Fig. 9 shows a general comparison of plants in both systems. Figs. 10, 11 depict a comparison of some plant samples from a side and top view. Tipburn incidence is observed in plant samples from System 1 due to excessive supplemental

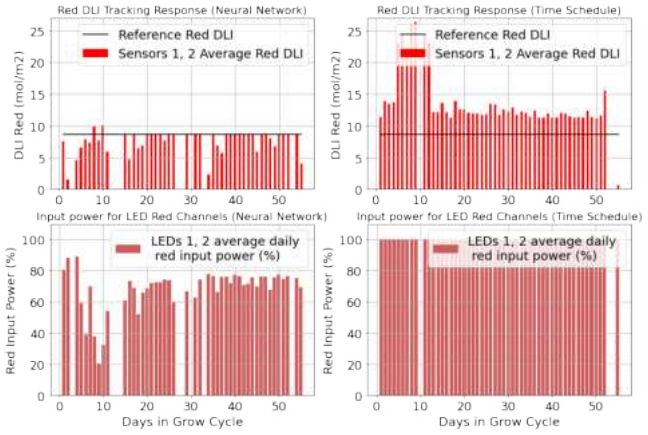

FIGURE 6. Red DLI tracking response for neural-network and time scheduling controllers.

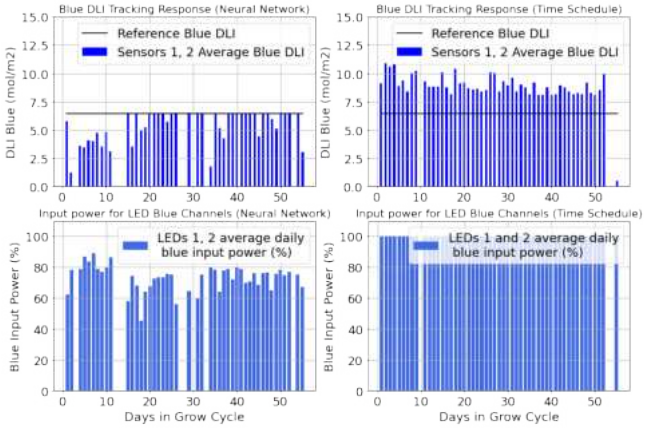

FIGURE 7. Blue DLI tracking response for neural-network and time scheduling contrllers.

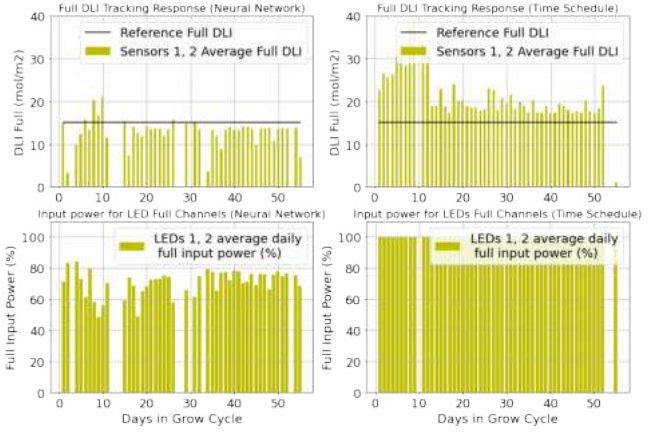

FIGURE 8. Full DLI tracking response for neural-network and time scheduling controllers.

FIGURE 9. General comparison of plants in both systems.

FIGURE 10. Top view comparison of plant samples.

FIGURE 11. Side view comparison of plant samples.

lighting. Tipburn is a serious problem in lettuce production under artificial illumination, which occurs as a result of decreasing calcium concentrations in the leaves [40], [41]. This problem is avoided in System 2 by producing a uniform PPFD at plant canopy level.

About 40% of the crop were selected randomly as samples to conduct comparative measurements of fresh and dry weights. The selected plant samples were cut from the stem

Sum of Weights (g)				
System (Method)	Full Plant Sample Fresh	Full Plant Sample Dry	Leaf Sample Fresh	Leaf Sample Dry
System 1 (TS)	582	37	14	7
System 2 (NN)	450	32	19	7
Average Weights (g)				
System-Method	Full Plant Sample Fresh	Full Plant Sample Dry	Leaf Sample Fresh	Leaf Sample Dry
System 1 (TS)	116	7	3	1
System 2 (NN)	90	6	4	1

TABLE 7. Comparison of fresh and dry weights of plants and leaf samples (NN: Neural Network; TS: Time Scheduling).

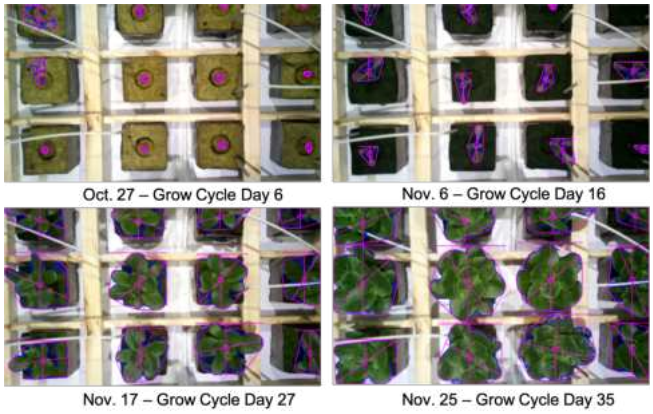

FIGURE 12. Neural-network controller plant Images processed for 4 random days (Oct 27, Nov 6, Nov 17, Nov 25) throughout the growth cycle.

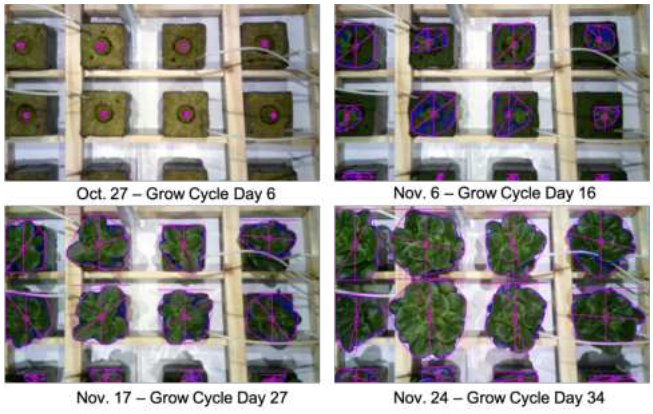

FIGURE 13. Time scheduling controller plant images processed for 4 random days (Oct 27, Nov 6, Nov 17, Nov 25) throughout the growth cycle.

and fresh weighs were recorded immediately. To record the dry weights, the YAMATO DX 402 Drying Oven was used and the samples were dried for 48 hours at $105°C$. From each plant sample, a leaf sample was collected, weighed, and scanned.

The results of weight measurements between the two systems are shown in Table 7, according to which the total fresh weight for plant samples of System 1 was 23% higher than that of samples of System 2. For the collected leaf samples, however, samples of System 2 have 26% higher fresh weight than System 1.

Fresh weight is not a reliable indicator for comparing yield after applying any treatments. Dry weight on the other hand, provides a precise measurement of biomass, eliminating fluctuations caused by water content because the drying process eliminates water from the plant. The plant total biomass can be directly related to our plant performance in response to factors such as photosynthetic capacity, nutrition, and environmental conditions. This is why dry weight is the best option to record weight when evaluating treatments in terms of yield or quality [42], [43].

Referring to Table 7, the dry weight of plant samples of System 1 are just 14% higher than those of System 2. Leaf samples of System 2 have 4% higher dry weights than System 1. Comparing the dry weight results for the two systems, dry weight of plant samples in System 2 was decreased by 14%, whereas the dry weight of leaf samples of this system was increased by 4%. This result is consistent with the improvements observed in plant quality and energy savings, compared to a non-significant weight increase.

D. PLANT GROWTH INDICATORS THROUGH VISUAL MONITORING

Plant area and plant leaf area are shown to have a direct relationship with plant health and yield. In an attempt to quantify this relationship, periodic top view images were captured at different times of day under white light conditions. The PlantCV open source software was used to process these images and extract some features indicative of plant growth. These indicators only work until the plant canopies start to overlap (November 25th-day 35 for NN system and November 24th-day 34 for TS system). Figures 12 and 13 illustrate the results of shape analysis performed on collected plant images of Systems 1 and 2, respectively. The shape analysis is a tool used to extract shape characteristics of a plant image, including height, object area, convex hull, convex hull area, and perimeter.

In Fig. 14, a comparison of convex hull measurements for plants in Systems 1 and 2 is shown. This feature indicates the plant growth process. Some inaccuracies in the color-based plant segmentation method occurred as a result of the green hue of the wool blocks and algae growth on the block surfaces, resulting in erroneous measurement peaks throughout the cycle. Plants 6 and 7 were the only ones that are in full view in both systems throughout the cycle. Comparing the corresponding figures, a slightly faster growth and higher plant area is observed for System 1, which is in agreement with the findings in section VI.C.

E. ENERGY SAVINGS PER UNIT OF DRY BIOMASS

The energy usage for the full growth cycle with D days for each of Systems 1 and 2 denoted by $E_{c,j}$ $(j = 1,\ 2)$ can be

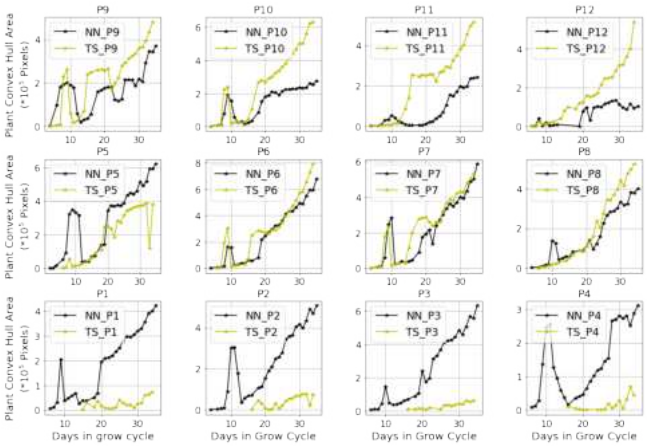

FIGURE 14. Comparison of the two controllers in terms of convex hull area of plants in pixels (growth cycle days 1 to 34). NN: Neural Network Controller; TS: Time Scheduling Controller.

calculated as follows

$$E_{c,j} = \sum_{d=1}^{D} E_{d,j} \tag{11}$$

where the daily energy usage $E_{d,j}$ $(j = 1, 2)$ can be formulated as follows

$$E_{d,j} = E_{d,r,j} + E_{d,b,j} \tag{12}$$

$$E_{d,r,j} = \sum_{i=0}^{n} E_{d,r,j,i} = \sum_{i=0}^{n} \sum_{t=0}^{T_p \times 3600} u_{r,j,i}(t) \times P_r \tag{13}$$

$$E_{d,b,j} = \sum_{i=0}^{n} E_{d,b,j,i} = \sum_{i=0}^{n} \sum_{t=0}^{T_p \times 3600} u_{b,j,i}(t) \times P_b \tag{14}$$

in which $E_{d,r,j}$ and $E_{d,b,j}$ are the red and blue channel energy usage of system j in day d, respectively; T_p is the photoperiod; $u_{r,j,i}$ and $u_{b,j,i}$ are the red and blue LED channel commands (dimming percentages), respectively; and $P_r = 14W$ and $P_b = 7W$ are the full power usage of each color channel of the light fixtures, respectively.

Based on formulations in (11), (12), (12), and (13), the energy usage for each system throughout the full 45-day grow cycle is calculated as follows

$$E_{c,1} = E_{c,r,1} + E_{c,b,1} = 17 + 9 = 26\ KWh \tag{15}$$

$$E_{c,2} = E_{c,r,2} + E_{c,b,2} = 11 + 6 = 17\ KWh \tag{16}$$

which shows that during the entire cycle, energy savings of 40% in the red spectrum and 35% in the blue spectrum were achieved, respectively, which corresponds to a net 38% electric energy saving.

As discussed in section VI.C, despite the significant energy savings achieved by System 2, the dry weight of lettuce grown in System 1 was 14% percent higher than that of System 2. To make meaningful comparisons between the two systems, parameters such as dry biomass produced per kWh and energy consumption per unit dry mass are presented in Table 8. These results demonstrate that 40% more dry biomass was produced per kWh and energy consumption per unit dry mass of lettuce was reduced by 28% using the proposed neural-network controller compared to the time scheduling technique.

TABLE 8. Relationship Between Plant Dry Weights and Their Respective Energy Consumption

Growth Parameter	Time Scheduling	Neural Network
Dry weight (g)	37	32
Energy Consumption (kWh)	26	16
Energy per unit Dry weight (kWh/g)	0.7	0.5
Conversion Efficiency (g/kWh)	1	2

VI. CONCLUSIONS

Experimental results demonstrate that the proposed approach can reduce energy consumption per unit dry mass of lettuce when compared to the conventional time scheduling technique and ameliorate certain plant health issues related to excessive light intensity. The proposed system demonstrates improvements that can be achieved through controlling and maintaining a desired lighting profile during the crop growth phases but challenges remain. For instance, strategic placement of light sensors throughout the plant canopy must be addressed due to sensor shading by plants' leaves. Combining image data with sensor data to identify the correct amount of light that each plant receives could be one approach to address this challenge.

For many years, red and blue color channels have been the spectra of choice for horticultural LEDs due to their photosynthetic efficiency and well understood effects on the plant growth process. However, recent studies have highlighted the importance of lesser-understood light spectra, including UV, green, and far-red lights. Thus, LED technologies that permit independent manipulation of narrow spectral components can be utilized to manipulate the light wavelengths to achieve desired plant properties.

Finally, supplemental lighting for photosynthesis in greenhouses can impact spatial distributions of temperature, relative humidity, water vapor pressure deficit, air movement, and CO_2 concentration. The study of these relationships through establishment of an ecosystem comprised of various environmental sensors and actuators is a potential area of future research. For each specific case, a multi-objective optimization problem can be defined based on plant requirements, resource availability, and cost, to optimize resource use efficiency, and plant quality and quantity.

ACKNOWLEDGMENT

The authors would like to thank Andres Torres, MSc, Research Greenhouse Coordinator and Deborah Henderson, PhD, Director, of the Institute for Sustainable Horticulture, Kwantlen Polytechnic University for facilitating the plant experiments.

REFERENCES

[1] S. Hemming, "Use of natural and artificial light in horticulture-interaction of plant and technology," in *VI International Symposium on Light in Horticulture 907*, 2009, pp. 25–35.

[2] K. J. McCree, "The action spectrum, absorptance and quantum yield of photosynthesis in crop plants," *Agricultural Meteorology*, vol. 9, pp. 191–216, 1971.

[3] C. Barnes, T. Tibbitts, J. Sager, G. Deitzer, D. Bubenheim, G. Koerner, and B. Bugbee, "Accuracy of quantum sensors measuring yield photon flux and photosynthetic photon flux," *HortScience*, vol. 28, no. 12, pp. 1197–1200, 1993.

[4] R. C. Morrow, "Led lighting in horticulture," *HortScience*, vol. 43, no. 7, pp. 1947–1950, 2008.

[5] L. Marcelis, F. Maas, and E. Heuvelink, "The latest developments in the lighting technologies in dutch horticulture," in *IV International ISHS Symposium on Artificial Lighting 580*, 2000, pp. 35–42.

[6] E. Heuvelink and H. Challa, "Dynamic optimization of artificial lighting in greenhouses," in *International Symposium on Growth and Yield Control in Vegetable Production 260*, 1989, pp. 401–412.

[7] L. Albright, A. Both, and A. J. Chiu, "Controlling greenhouse light to a consistent daily integral," *Transactions of the ASAE*, vol. 43, pp. 421–431, 03 2000.

[8] R. Moe, "Physiological aspects of supplementary lighting in horticulture," in *III International Symposium on Artificial Lighting in Horticulture 418*, 1994, pp. 17–24.

[9] T. Kozai, *Why LED Lighting for Urban Agriculture?* Singapore: Springer Singapore, 2016, pp. 3–18.

[10] Y. Xu, Y. Chang, G. Chen, and H. Lin, "The research on led supplementary lighting system for plants," *Optik - International Journal for Light and Electron Optics*, vol. 127, no. 18, pp. 7193 – 7201, 2016.

[11] T. Ouzounis, E. Rosenqvist, and C.-O. Ottosen, "Spectral effects of artificial light on plant physiology and secondary metabolism: A review," *HortScience*, vol. 50, no. 8, pp. 1128–1135, 2015.

[12] A. Viršilė, M. Olle, and P. Duchovskis, "Led lighting in horticulture," in *Light emitting diodes for agriculture*. Springer, 2017, pp. 113–147.

[13] G. D. Massa, H.-H. Kim, R. M. Wheeler, and C. A. Mitchell, "Plant productivity in response to led lighting," *HortScience*, vol. 43, no. 7, pp. 1951–1956, 2008.

[14] L. Bachouch, P. Dupuis, N. Sewraj, L. Canale, G. Zissis, L. Bouslimi, and L. E. Amraoui, "Tunable multiple-leds combination spectrum for plants based on mccree par spectrum," in *2020 IEEE International Conference on Environment and Electrical Engineering and 2020 IEEE Industrial and Commercial Power Systems Europe (EEEIC / ICPS Europe)*, 2020, pp. 1–6.

[15] L. Sipos, I. F. Boros, L. Csambalik, G. Székely, A. Jung, and L. Balázs, "Horticultural lighting system optimalization: A review," *Scientia Horticulturae*, vol. 273, p. 109631, 2020. [Online]. Available: https://www.sciencedirect.com/science/article/pii/S0304423820304593

[16] L. Sipos, I. F. Boros, L. Csambalik, G. Székely, A. Jung, and L. Balázs, "Horticultural lighting system optimalization: A review," *Scientia Horticulturae*, vol. 273, p. 109631, 2020.

[17] P. Pinho, T. Hytönen, M. Rantanen, P. Elomaa, and L. Halonen, "Dynamic control of supplemental lighting intensity in a greenhouse environment," *Lighting Research & Technology*, vol. 45, no. 3, pp. 295–304, 2013.

[18] T. Schwend, M. Beck, D. Prucker, S. Peisl, H. Mempel *et al.*, "Test of a par sensor-based, dynamic regulation of led lighting in greenhouse cultivation of helianthus annuus," *Eur J Hortic Sci*, vol. 81, pp. 152–156, 2016.

[19] G. Cocetta, D. Casciani, R. Bulgari, F. Musante, A. Kołton, M. Rossi, and A. Ferrante, "Light use efficiency for vegetables production in protected and indoor environments," *The European Physical Journal Plus*, vol. 132, no. 1, pp. 1–15, 2017.

[20] C. Lork, M. Cubillas, B. K. K. Ng, C. Yuen, and M. Tan, "Minimizing electricity cost through smart lighting control for indoor plant factories," in *IECON 2020 The 46th Annual Conference of the IEEE Industrial Electronics Society*. IEEE, 2020, pp. 297–302.

[21] L. Poulet, G. Massa, R. Morrow, C. Bourget, R. Wheeler, and C. Mitchell, "Significant reduction in energy for plant-growth lighting in space using targeted led lighting and spectral manipulation," *Life Sciences in Space Research*, vol. 2, pp. 43 – 53, 2014.

[22] C.-L. Chang, G.-F. Hong, and Y.-L. Li, "A supplementary lighting and regulatory scheme using a multi-wavelength light emitting diode module for greenhouse application," *Lighting Research & Technology*, vol. 46, no. 5, pp. 548–566, 2014.

[23] D. Durmus, "Real-time sensing and control of integrative horticultural lighting systems," *J*, vol. 3, no. 3, pp. 266–274, 2020.

[24] C. Gómez and L. G. Izzo, "Increasing efficiency of crop production with leds," *AIMS Agriculture and Food*, vol. 3, no. 2, pp. 135–153, 2018.

[25] D. Piromalis, K. Arvanitis, P. Papageorgas, and K. Ferentinos, "Smart precision lighting for urban and landscape closed controlled horticultural environments," in *Urban Horticulture*. Springer, 2018, pp. 107–140.

[26] C. Nicole, F. Charalambous, S. Martinakos, S. Van De Voort, Z. Li, M. Verhoog, and M. Krijn, "Lettuce growth and quality optimization in a plant factory," in *VIII International Symposium on Light in Horticulture 1134*, 2016, pp. 231–238.

[27] R. Sowmya, S. Narasimhan, C. P. Kurian, and R. Srividya, "Metabolic variations in grass c. dactylon and selection of optimal leds for the horticulture luminaire using lm algorithm," *IEEE Access*, vol. 9, pp. 139 457–139 465, 2021.

[28] D. Xu, Q. Yang, Y. Tong, and L. G. van Willigenburg, "Optimal control of led light intensity in a plant factory," in *2020 39th Chinese Control Conference (CCC)*, 2020, pp. 1362–1367.

[29] Z. Tian, W. Ma, Q. Yang, and F. Duan, "Research status and prospect of energy-saving technology of led light source in plant factory," in *2020 17th China International Forum on Solid State Lighting 2020 International Forum on Wide Bandgap Semiconductors China (SSLChina: IFWS)*, 2020, pp. 152–158.

[30] C. Lork, M. Cubillas, B. K. Kiat Ng, C. Yuen, and M. Tan, "Minimizing electricity cost through smart lighting control for indoor plant factories," in *IECON 2020 The 46th Annual Conference of the IEEE Industrial Electronics Society*, 2020, pp. 297–302.

[31] J. Jiang, A. Mohagheghi, and M. Moallem, "Energy-efficient supplemental led lighting control for a proof-of-concept greenhouse system," *IEEE Transactions on industrial electronics*, vol. 67, no. 4, pp. 3033–3042, 2019.

[32] A. Mohagheghi and M. Moallem, "Intelligent spectrum controlled supplemental lighting for daylight harvesting," *IEEE Transactions on Industrial Informatics*, vol. 17, no. 5, pp. 3263–3272, 2020.

[33] A. Ryer and V. Light, "Light measurement handbook," 1997.

[34] Johnny. (2022) Johnnys Selected Seeds dragoon organic lettuce seed. [Online]. Available: https://www.johnnyseeds.com/vegetables/lettuce/dragoon-organic-lettuce-seed-3884G.html?cgid=lettuce

[35] D. Loconsole and P. Santamaria, "Uv lighting in horticulture: A sustainable tool for improving production quality and food safety," *Horticulturae*, vol. 7, no. 1, p. 9, 2021.

[36] A. Both, L. Albright, R. Langhans, R. Reiser, and B. Vinzant, "Hydroponic lettuce production influenced by integrated supplemental light levels in a controlled environment agriculture facility: Experimental results," in *III International Symposium on Artificial Lighting in Horticulture 418*, 1994, pp. 45–52.

[37] C. Piovene, F. Orsini, S. Bosi, R. Sanoubar, V. Bregola, G. Dinelli, and G. Gianquinto, "Optimal red: blue ratio in led lighting for nutraceutical indoor horticulture," *Scientia Horticulturae*, vol. 193, pp. 202–208, 2015.

[38] R. Paradiso and S. Proietti, "Light-quality manipulation to control plant growth and photomorphogenesis in greenhouse horticulture: The state of the art and the opportunities of modern led systems," *Journal of Plant Growth Regulation*, pp. 1–39, 2021.

[39] A. Abbasi and N. Fahlgren, "Naïve bayes pixel-level plant segmentation," in *2016 IEEE Western New York Image and Signal Processing Workshop (WNYISPW)*, Nov 2016, pp. 1–4.

[40] Y. Sago, "Effects of light intensity and growth rate on tipburn development and leaf calcium concentration in butterhead lettuce," *HortScience*, vol. 51, no. 9, pp. 1087–1091, 2016.

[41] L. Gaudreau, J. Charbonneau, L.-P. Vézina, and A. Gosselin, "Photoperiod and photosynthetic photon flux influence growth and quality of greenhouse-grown lettuce," *HortScience*, vol. 29, no. 11, pp. 1285–1289, 1994.

[42] W. Huang, D. A. Ratkowsky, C. Hui, P. Wang, J. Su, and P. Shi, "Leaf fresh weight versus dry weight: which is better for describing the scaling relationship between leaf biomass and leaf area for broad-leaved plants?" *Forests*, vol. 10, no. 3, p. 256, 2019.

[43] Hortamericas. (2022) Fresh weight vs. dry weight. [Online]. Available: https://hortamericas.com/blog/fresh-weight-vs-dry-weight/

AFAGH MOHAGHEGHI (Student Member, IEEE) received the B.Sc. and M.Sc. degrees in electrical engineering and control systems from Shiraz University, Shiraz, Iran, in 2008 and 2010, respectively; and the Ph.D. degree in Mechatronic Engineering from Simon Fraser University, Canada, in 2022. From 2012 to 2016, she held research and faculty positions with Shiraz University and Marvdasht Azad University, Shiraz, Iran. Her research interests include intelligent control, sustainable energy systems, Internet-of-Things enabled systems, and applications of data science and machine learning.

MEHRDAD MOALLEM (Member, IEEE) received the Ph.D. degree in electrical and computer engineering from Concordia University, Montreal, QC, Canada, in 1997. From 1997 to 2007, he held research and faculty positions at Concordia University, Duke University, Durham, NC, USA, and The University of Western Ontario, London, ON, Canada. He joined Fraser University, Canada, in 2007, where he is currently Professor of Mechatronic Systems Engineering. His research interests include multidisciplinary areas related to control applications including mechatronics, energy systems, and power electronics. He has served on the editorial boards of several conferences and journals including the American Control Conference, IEEE/ASME Transactions on Mechatronics, and IFAC Journal of Mechatronics.